ACS SyntheticBiology

Research Article

pubs.acs.org/synthbio

Stochasticity in Gene Expression in a Cell-Sized Compartment

Kazuya Nishimura,[†,‡] Saburo Tsuru,[†] Hiroaki Suzuki,[§,∥] and Tetsuya Yomo*[,†,∥,⊥]

[†]Department of Bioinformatic Engineering, Graduate School of Information Science and Technology, Osaka University, Yamadaoka 1-5, Suita, Osaka 565-0871, Japan

[‡]Quantitative Biology Center (QBiC), Riken, Fuedai 6-2-3, Suita, Osaka 565-0874, Japan

[§]Faculty of Science and Engineering, Chuo University, Kasuga 1-13-27, Bunkyo-ku, Tokyo 112-8551, Japan

[∥]Exploratory Research for Advanced Technology (ERATO), Japan Science and Technology Agency, Yamadaoka 1-5, Suita, Osaka 565-0871, Japan

[⊥]Department of Frontier Biosciences, Graduate School of Frontier Biosciences, Osaka University, Yamadaoka 1-5, Suita, Osaka 565-0871, Japan

Supporting Information

ABSTRACT: The gene expression in a clonal cell population fluctuates significantly, and its relevance to various cellular functions is under intensive debate. A fundamental question is whether the fluctuation is a consequence of the complexity and redundancy in living cells or an inevitable attribute of the minute microreactor nature of cells. To answer this question, we constructed an artificial cell, which consists of only necessary components for the gene expression (*in vitro* transcription and translation system) and its boundary as a microreactor (cell-sized lipid vesicle), and investigated the gene expression noise. The variation in the expression of two fluorescent proteins was decomposed into the components that were correlated and uncorrelated between the two proteins using a method similar to the one used by Elowitz and co-workers to analyze the expression noise in *E. coli*. The observed fluctuation was compared with a theoretical model that expresses the amplitude of noise as a function of the average number of intermediate molecules and products. With the assumption that the transcripts are partly active, the theoretical model was able to well describe the noise in the artificial system. Furthermore, the same measurement for *E. coli* cells harboring an identical plasmid revealed that the *E. coli* exhibited a similar level of expression noise. Our results demonstrated that the level of fluctuation found in bacterial cells is mostly an intrinsic property that arises even in a primitive form of the cell.

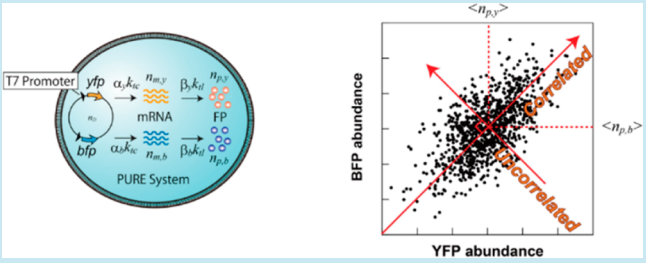

KEYWORDS: *artificial cell, fluctuation, gene expression*

Biological cells essentially consist of the lipid membrane that surrounds cytosolic components for metabolic reactions, which all occur within a small space on the order of a femtoliter (10^{-15} L). Thus, unlike the large-scale test tube used in biochemistry, the reactions in cells are subjected to fluctuations in both the environmental factors and the molecular number of their own components. As a result, the biochemical reactions essential for cell survival and activities, such as gene expression, exhibit significant fluctuations, or noise, even in a clonal population.[1−5] Although this noise seems to obscure the precise regulation of cellular behaviors, it is now widely accepted that noise is not merely an impediment but often drives many essential cell activities, such as evolution, development, adaptation, stress responses, cell cycle, circadian rhythms, and aging.[6−9] However, it is often difficult to pin down the origin of the fluctuation observed in cells because cells have numerous different components that may or may not affect the property of interest and because these cells as microreactors are subjected to the dynamics of growth and division.[10] To avoid the obstacles caused by the complicacy in cells, artificial or synthetic cells have been devised using a bottom-up approach to understand the essential properties of cells.[11−16] To date, various key features of cells have been modeled and tested experimentally using only a minimal set of molecular components; these features include the occurrence of gene expression reactions,[17−20] the amplification and self-reproduction of genetic molecules,[21−24] and the growth and division of the cellular membrane.[25−31] Surprisingly, some phenomena that resemble the functions of living cells are found in the artificial systems.[32,33] In addition to making progress in this field, some researchers began to look into the fluctuations that arise in the artificial cell mimics. For instance, the size of the lipid vesicles that are used as cellular containers varies widely when the vesicles are formed via a spontaneous assembly process.[34−36] Large fluctuations are reported in the metabolic reactions, such as the gene expression that occurs in

Received: May 15, 2014
Published: October 3, 2014

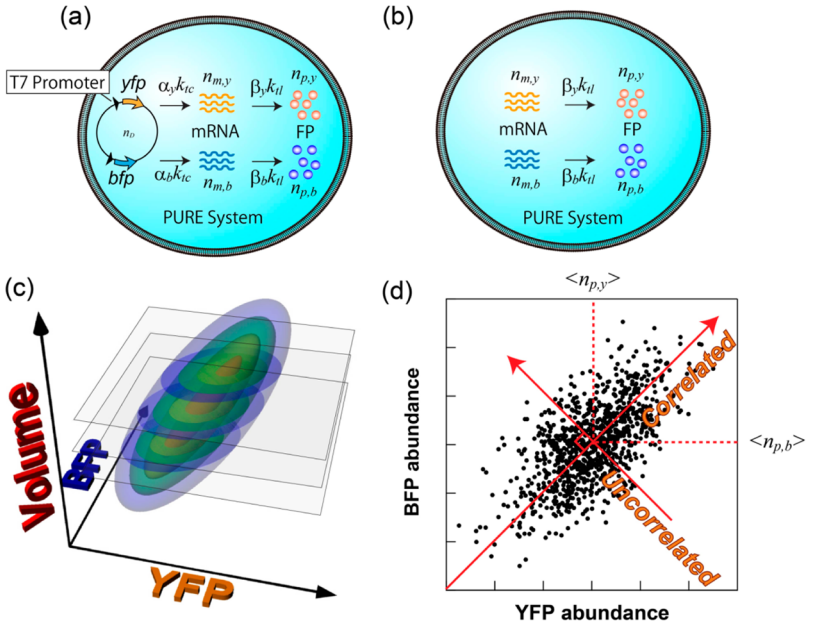

Figure 1. Schematics of the artificial cell system and analysis. (a) The transcription and translation reaction for synthesizing two fluorescent proteins (FPs, *i.e.*, YFP and BFP) encoded on the plasmid DNA. (b) The translation reaction for synthesizing two FPs encoded on the separate mRNAs. Both reactions are enclosed in giant vesicles. See the text for nomenclature. (c) Schematic for the typical 3D density plot for the obtained data. Vesicles fluctuate in the volume and two synthesized FPs. (d) Example of the scatterplot for two FPs in vesicles with identical volume. Abundances of FPs in individual vesicles fluctuate in correlated and uncorrelated contributions, which correspond to the variations parallel and perpendicular, respectively, to the diagonal line.

encapsulated in vesicles, of a population; the reasons for these fluctuations remain unknown.[37] Recently, the noise in gene expression was measured and analyzed using an *in vitro* transcription and translation system enclosed in 20 fL microchambers.[38] The researchers reported unexpected behavior in which the noise deviated from the simple Poissonian assumption and deduced that the noise originated from translational bursting. However, studies of the fluctuations in artificially constructed cell mimics are still in their infancy, and detailed investigations are required.

In this study, we investigated the gene expression noise in cell-sized lipid vesicles we have been studied for a decade as artificial cell mimics. We employed a dual reporter system which Elowitz and co-workers had devised to study the contribution of the intrinsic and extrinsic noise components of gene expression in living cells.[1] As the transcription and translation reaction proceeded, two fluorescent proteins (FPs) of different colors were coexpressed; these FPs were encoded on the same plasmid under distinct promoters. The abundances of the FPs fluctuated among the vesicle population, and the total variance was decomposed into the components that were correlated between the two FPs and those that were not. We introduced a theoretical formulation predicting the contribution of these components under a set of average reaction rates, which could be determined experimentally. Comparing the experimental result and the model revealed the mechanism of the noise generation in the gene expression that occurred in the cell-sized vesicles. We also measured the expression using the same plasmid DNA in a biological cell, *Escherichia coli* (*E. coli.*), to compare the noise in the artificial cell with that in the living cell. We found that the artificial cell had less correlated noise because of the smaller vesicle-to-vesicle variation in the reaction rate; this variation has global effects. However, the amplitude of the uncorrelated noise was similar in the artificial and living cells, perhaps because stochasticity in the translation and transcription steps is unavoidable. The stochasticity seems to have been viable even in primordial cells, thus allowing for further evolution of various biological properties.

RESULTS AND DISCUSSION

Experimental Design. To evaluate the noise in the artificial cell, we measured the fluctuations in the amount of the two FPs within individual cell-sized vesicles; the two FPs were synthesized via a gene expression reaction. For this experiment, we prepared cell-sized vesicles containing an *in vitro* transcription and translation system (PURE system),[39−41] together with the plasmid DNA that codes either yellow fluorescent protein (YFP) and blue fluorescent protein (BFP) under distinct copies of the T7 promoter (Figure 1a). As the reaction proceeded, the two genes were transcribed into mRNAs, which were then translated into reporter FPs. We also prepared vesicles containing the mRNAs that code for either reporter FP (Figure 1b) to evaluate the noise that arises in the translation step. In addition to the reaction system, these vesicles contained purified red FP (Transferrin Alexa Fluor 647 Conjugate, Molecular Probes) as a marker for estimating the vesicle volume. The intensities from three FPs in individual vesicles were measured using a fluorescence flow cytometer (FCS; BD FACS Aria). The amount of the reporter FPs in the vesicles was obtained from the fluorescence intensities (FIs) via the corresponding conversion factors (see Methods section). The red FI was converted to the vesicle volume V (i.e., size of the reaction container) by multiplying the conversion factor obtained from a FI measurement of calibration beads that have a known amount of red FP.

The typical measurement data are represented schematically in Figure 1c as a 3D density map of the frequency of the vesicles. The individual vesicles fluctuate in three dimensions:

dx.doi.org/10.1021/sb500249g | *ACS Synth. Biol.* 2015, 4, 566−576

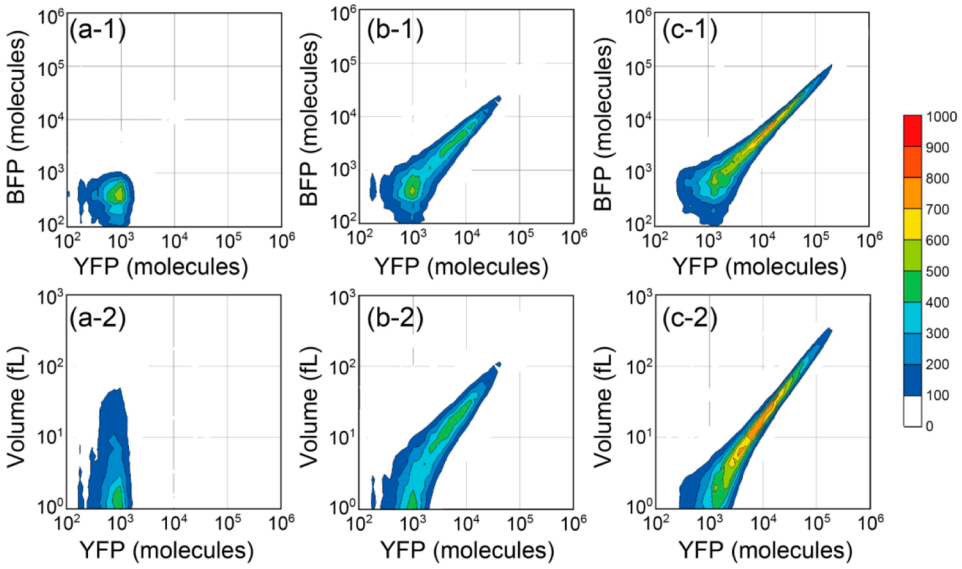

Figure 2. 2D contour plots of the measurement data for the transcription and translation reaction with 1 nM plasmid DNA. (a) In vesicle reaction before incubation. (b) In vesicle reaction after 240 min incubation. (c) In tube reaction product encapsulated in vesicles (postreaction encapsulation). Upper figures show plots for YFP and BFP, and lower figures show plots for YFP and volume (projections onto the YFP−BFP plane and YFP−volume plane in Figure 1a, respectively). The color bar represents the frequency of vesicles in the logarithmic bins.

vesicle volume and the abundances of YFP and BFP. In principle, the abundances of the synthesized FPs increased proportionally to the vesicle volume; thus, in 3D space, the densest contour region stretched at a certain angle with respect to the YFP-BFP plane. Furthermore, even in the vesicles with identical volume, the abundances of the synthesized FPs fluctuated stochastically. When an iso-volume plane is extracted from the 3D density plot, we obtain the scatter plot for YFP and BFP, as exampled in Figure 1d. The variations in the two synthesized FPs characterize the contributions of different aspects of the cellular system to the gene expression; these aspects are represented by the correlated and uncorrelated noise components.[1,42,43] In short, the correlated noise represents the variation in the overall activity of gene expression; thus, it appears as the variance that is parallel to the diagonal line (the line crossing the origin and the means of the two FPs). The uncorrelated noise represents stochasticity in the biochemical process of gene expression, which is not correlated between the two FPs. Thus, this component appears as the variance that is perpendicular to the diagonal line. The correlated and uncorrelated noise components make orthogonal contributions to the total noise.

Measurement of Gene Expression in the Artificial Cell. In practice, we prepared cell-sized vesicles containing the *in vitro* transcription and translation system and the plasmid DNA coding the two FPs (Figure 1a) using the water-in-oil emulsion transfer method, which allows direct encapsulation of the reaction solution.[39,44−46] All preparation steps were conducted below 4 °C, and the gene expression reaction was initiated by incubating the final vesicles suspension at 37 °C. The tested DNA concentrations were 0.33, 1, 3, and 9 nM, which correspond to 0.2, 0.6, 1.8, and 5.4 molecule/fL (DNA start reaction). During the incubation, small aliquots (2 μL) of the vesicle suspension were sampled every 30 min and were measured using FCS. The volume of the main population of vesicles ranged from 1 to 50 fL, which was barely affected by either the encapsulated solution or the incubation (Supporting Information Figure S1). Typical measurement data for the 1 nM plasmid DNA condition are shown in Figure 2 (the results for 0.33, 3, and 9 nM DNA are shown in Figure S2). The abundances of the reporter FPs (YFP and BFP) were negligible before the incubation (within the background level, Figure 2(a-1)). Then, they increased as the synthesis reaction proceeded (Supporting Information Figure S3). The abundances of the FPs saturated due to the gradual inactivation of the system, which occurred before 240 min in all experimental conditions. An increase in the reporter FPs that was significantly greater than the background level was observed for vesicle volumes that were typically larger than ∼10 fL (Figure 2 a, b lower figures). Thus, in the later sections, we analyzed the data obtained from the 240 min incubation for a volume range from 7 to 83 fL. For the control experiment, we prepared vesicles containing the same inner solution, but the reaction was completed in a test tube prior to encapsulation into the vesicles (hereafter postreaction encapsulation) to evaluate the measurement noise (Figure 2c). We also conducted the same procedures for vesicles containing mRNAs that coded either YFP and BFP (Figure 1b) at concentrations of 33, 100, 300, and 900 nM (concentration of total mRNA), which correspond to 20, 60, 180, and 540 molecules/fL (Supporting Information Figure S4). As mentioned earlier, the abundance of the synthesized FPs was dependent on the vesicle volume; more FPs were synthesized in the larger reaction container for the same DNA concentration.

Thus, we separated the data based on the vesicle volume into logarithmic bins having $(\log_{10} 2)/4$ width and conducted the analysis. This operation is equivalent to sectioning the data into the iso-volume plane depicted in Figure 1c. We confirmed that the width of this binning window was sufficiently narrow to not affect the amplitude of the noise (Supporting Information Figure S5). First, we examined whether the encapsulation into the vesicles altered the transcription and translation reactions. We calculated the mean concentration of each FP at 240 min, that is, $\overline{n_{p,y}}/V$ and $\overline{n_{p,b}}/V$ in every volume bin, where $\overline{n_{p,y}}$ and $\overline{n_{p,b}}$ are the average number of yfp and bfp proteins in a vesicle, and V represents the vesicle volume in the sectioned data set.

dx.doi.org/10.1021/sb500249g | *ACS Synth. Biol.* 2015, 4, 566−576

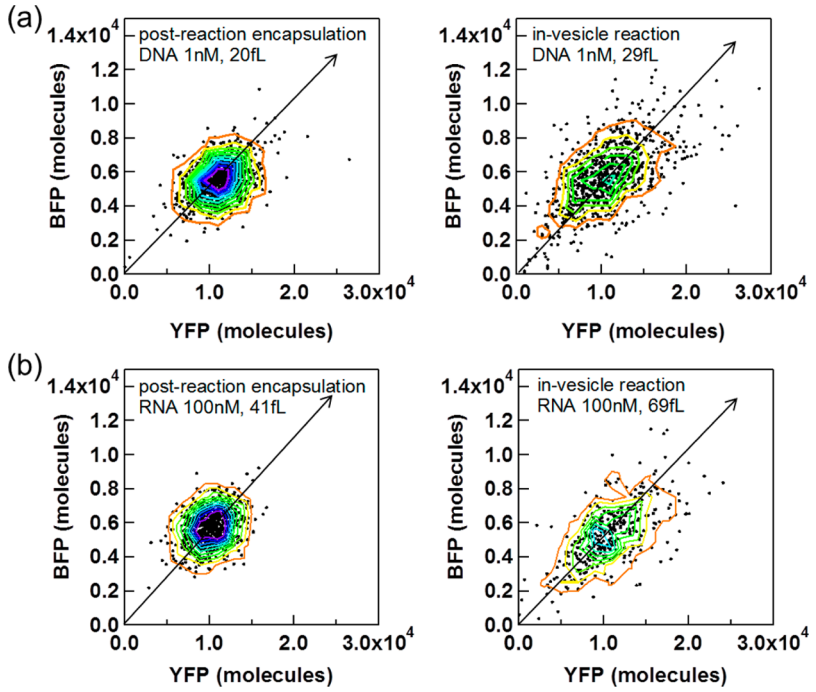

Figure 3. Scatter and contour plots showing the correlation of YFP and BFP abundances in individual vesicles sectioned at the iso-volume plane. Sections with the mean protein abundance ~6000 were shown. (a) DNA 1 nM. (b) RNA 100 nM. Arrowhead line is the diagonal line.

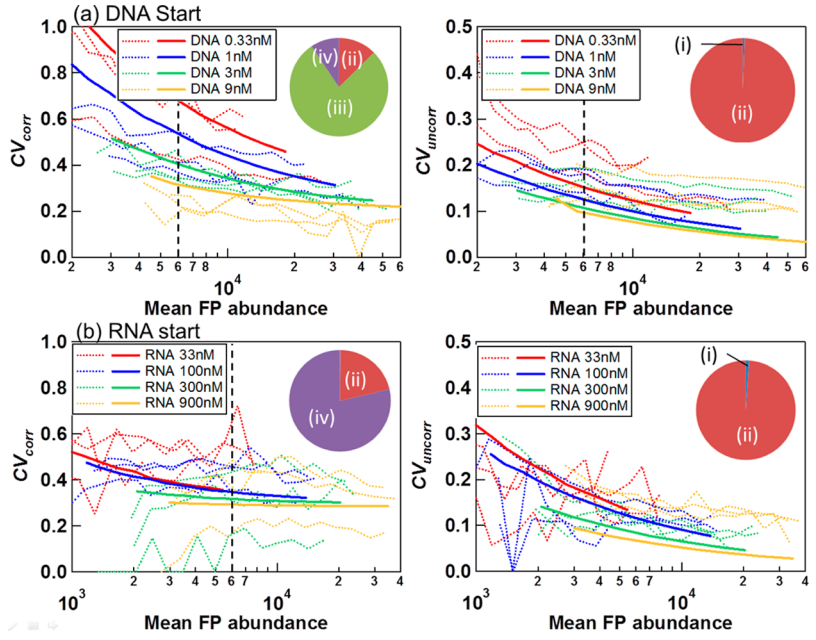

Figure 4. Correlated and uncorrelated noise in CV. (a) Noises in DNA start reaction. (b) Noises in RNA start reaction. In all figures, dotted lines represent the noise calculated from the experimental data (each three lines in the same color is triplicated experiments). Bold solid lines represent the fitted curves of the theoretical model with the fitted parameters $\gamma_{RNA} = 0.03$ and $CV_{k_d} = 0.2$. Vertical dotted lines show the mean FP abundance ~6000, at which the measured mean values are listed in Table 1. Insets show the relative contributions to the noise explained in eqs 5−8 in CV^2 for 0.33 nM DNA and 100 nM RNA start reactions. (i) the Poisson noise in translation, (ii) the Poisson noise in transcription or RNA encapsulation, (iii) the Poisson noise in DNA encapsulation, and (iv) the vesicle-to-vesicle variation in the translation rate.

We confirmed that the mean concentrations were constant for the all of the calculated volume ranges (Supporting Information Figure S6a−d). Thus, the reaction did not depend on the vesicle size. We further confirmed that the concentrations of the synthesized FPs were nearly the same as those in the postreaction encapsulation vesicles (Supporting Information Figure S6e, f). These observations demonstrate that the protein synthesis reaction proceeded without inhibition in the vesicles, which was consistent with our previous report.[39]

Correlated and Uncorrelated Noise in Gene Expression. Next, we evaluated the noise in the FP abundances. Because we employed a dual reporter system, the total noise could be separated into the component with a global influence (correlated noise) and the component that arose stochastically

dx.doi.org/10.1021/sb500249g | ACS Synth. Biol. 2015, 4, 566−576

(uncorrelated noise). Graphically, the amplitudes of these noise components are visualized in the scatter plot for the two FPs. Examples of the scatter plots of YFP and BFP at certain iso-V planes are shown in Figure 3. Here, iso-V planes, in which nearly 6000 FPs were synthesized on average, are presented (similar scatter plots for the other experimental conditions are shown in Supporting Information Figure S7). The shape of the contour is steep and nearly circular for the postreaction encapsulation in the reactions initiated from DNA and from mRNA (Figure 3a, b left figures). This result indicates that the fluctuations in encapsulating thousands of YFP and BFP molecules are relatively small and that the encapsulation of the FPs is uncorrelated. In contrast, when the reaction was conducted in vesicles (Figure 3a, b right figures), the contour spread more in the directions that were parallel and perpendicular to the diagonal line. In particular, the shape of the contour was ellipsoidal with a major axis that stretched along the diagonal line. This observation indicates that the FP synthesis became stochastic in the vesicles and that some sources of the correlated noise component were present to some extent when the gene expression was conducted in vesicles.

Here, we asked how much of the fluctuation in the synthesized FPs arose during the transcription and translation steps. After 240 min of incubation, the concentration of the synthesized FPs was typically on the order of 1 μM, which corresponds to 600 molecules per fL. Thus, in the postreaction encapsulation, the vesicles larger than 10 fL contained more than 6000 FP molecules; we can then assume that the concentration of FPs should not fluctuate among the vesicles having the same volume. Therefore, the variation in the FPs observed in this control (Figure 3a, b left) was considered systematic noise that arose even when measuring vesicles with identical amount of FPs. We determined the gene expression noise in terms of the FP variance in the *in-vesicle* reaction, from which we subtracted the variance in the postreaction encapsulation vesicles that had the same mean FP concentration. The results are shown as dotted lines in Figure 4; the noise in the coefficient of variation (CV) on the vertical axis was plotted versus the mean FP abundance on the horizontal axis. In the DNA start reaction, the correlated component of the noise (CV_{corr}) decreased steeply as the amount of synthesized FPs increased (Figure 4a, left). Moreover, CV_{corr} also decreased as the initial concentration of plasmid DNA increased. The uncorrelated component (CV_{uncorr}) exhibited the similar trend, but dependence on the DNA concentrations was less significant (Figure 4a, right). In the RNA start reaction, the correlated noise remained nearly constant ($CV_{corr} \approx 0.2$) regardless of the mean FP and the initial RNA concentration (Figure 4b, left). The uncorrelated noise monotonically decreased with the mean FP abundance and almost became zero at large mean FP abundance (Figure 4b, right).

Theoretical Model for Predicting the Expression Noise. We introduced a theoretical model to evaluate the noise when the gene expression reaction is simplified into the sequential steps of plasmid DNA encapsulation, transcription, and translation. Following the basic concept and the logical flow presented by Swain et al.,[42] we construct the detailed formulation with fundamental reaction parameters. Here, we first considered the noise of a single FP and then derived the expressions for the correlated and uncorrelated noise components in the dual reporter system. Suppose that a vesicle contains plasmid DNA with a molecular abundance (number) n_D. The reporter gene is transcribed, and the copy number of mRNAs synthesized per a single gene during the incubation time is denoted as k_{tc}. Next, the mRNA is translated into the FP, and the copy number of FPs synthesized per a single mRNA during the incubation time is denoted as k_{tl}. These numbers may vary randomly among the vesicles because, for instance, the concentrations of encapsulated RNA polymerase and ribosome fluctuate among the vesicles. Under this circumstance, we consider the mean and variance of the synthesized FPs while assuming that each elemental step (encapsulation of DNA, transcription, and translation) follows an independent Poissonian process. Now, let us consider a vesicle population with identical volumes (*i.e.*, population in the iso-V plane); thus, the variance in the DNA copy number v_{n_D} is a simple random variable with a Poisson distribution, for example, $(v_{n_D}=\overline{n_D})$. Using these assumptions, we obtain the mean and variance, respectively, of the expressed FP as follows.

$$\overline{n_p} = \overline{k_{tl}k_{tc}n_D} \tag{1}$$

$$v_{n_p} = \overline{k_{tl}k_{tc}n_D} + \overline{k_{tc}n_D}(v_{k_{tl}} + \overline{k_{tl}}^2) + v_{n_D}(v_{k_{tc}} + \overline{k_{tc}}^2)(v_{k_{tl}} + \overline{k_{tl}}^2) + v_{k_{tc}}\overline{n_D}^2(v_{k_{tl}} + \overline{k_{tl}}^2) + v_{k_{tl}}\overline{n_D}^2\overline{k_{tc}}^2 \tag{2}$$

In this expression for v_{n_p}, the first through the third terms represent the Poisson noise in (i) translation, (ii) transcription amplified by the subsequent translation step, and (iii) the number of encapsulated DNAs amplified by the subsequent transcription and translation steps. The last two terms originate from (iv) the vesicle-to-vesicle variation in the transcription and translation activities.

Next, we consider the situation of a dual reporter system. For simplicity, we assume that there is no preference between synthesizing YFP or BFP in the reaction, that is, $\overline{n_{p,y}} = \overline{n_{p,b}}$, and $\overline{n_{m,y}} = \overline{n_{m,b}}$. The total variances of the two FPs, $v_{n_{p,y}} + v_{n_{p,b}}$, are decomposed into the correlated and uncorrelated components geometrically (see Supporting Information text). As a result, we find

$$v_{corr} = \overline{k_{tl}k_{tc}n_D} + \overline{k_{tl}}^2\overline{k_{tc}n_D} + 2\overline{k_{tl}}^2\overline{k_{tc}}^2\overline{n_D} + 2(\overline{k_{tl}}^2\overline{n_D} + \overline{k_{tl}}^2\overline{n_D}^2)v_{k_{tc}} + (\overline{k_{tc}}\overline{n_D} + 2\overline{k_{tc}}^2\overline{n_D} + 2\overline{k_{tc}}^2\overline{n_D}^2)v_{k_{tl}} + 2(\overline{n_D} + \overline{n_D}^2)v_{k_{tc}}v_{k_{tl}} \tag{3}$$

$$v_{uncorr} = \overline{k_{tl}k_{tc}n_D} + \overline{k_{tl}}^2\overline{k_{tc}n_D} + \overline{k_{tc}n_D}v_{k_{tl}} \tag{4}$$

Note that the noise from the number of DNA molecules (iii) only contributes to the correlated noise component v_{corr} (eq 3) because the genes of the two FPs are always on the same plasmid DNA. The noise components from the transcription and translation steps, (ii) and (i), are evenly distributed between v_{corr} (eq 3) and v_{uncorr} (eq 4) reflecting the independence between these steps for the two FPs. Moreover, the expression of v_{uncorr} (eq 4), the variance in the transcription rate $v_{k_{tc}}$, does not appear due to the identical copy number of the two FP genes in each vesicle. To compare the relative variation among the wide range of expression levels, eqs 3 and 4 are divided by the square of the mean FP abundance, that is, $\overline{n_p}^2$, to derive the square of the coefficient of variance, CV^2. As a result, we obtain

Table 1. List of Average Values in the In-Vesicle Reaction Determined from the Measurement

	V (fL)	n_D	n_m	n_p	k_{tc}	α_y	α_b	k_{tl}	β_y	β_b
DNA 0.33 nM	35.0	6.9	1791	6315	258.2	0.46	2.16	3.53	2.84	0.35
DNA 1 nM	20.8	12.5	2679	6342	214.4	0.45	2.20	2.37	2.92	0.34
DNA 3 nM	12.4	26.5	3622	5476	136.6	0.52	1.91	1.80	2.44	0.41
DNA 9 nM	8.8	47.3	3507	5618	74.2	0.72	1.38	1.60	1.64	0.61
RNA 100 nM	35.0		2102	5828				2.77	1.36	0.73
RNA 300 nM	24.8		4458	6057				1.36	1.29	0.78
RNA 900 nM	14.7		7953	5610				0.77	1.09	0.92

$$\mathrm{CV}^2_{\mathrm{corr}} = \frac{1}{\overline{k_{tl}}\,\overline{k_{tc}}\,\overline{n_D}} + \frac{1}{\overline{k_{tc}}\,\overline{n_D}}(\mathrm{CV}^2_{k_{tl}} + 1) + \frac{2}{\overline{n_D}}(\mathrm{CV}^2_{k_{tc}} + 1)(\mathrm{CV}^2_{k_{tl}} + 1) + 2\mathrm{CV}^2_{k_{tc}}(\mathrm{CV}^2_{k_{tl}} + 1) + 2\mathrm{CV}^2_{k_{tl}} \quad (5)$$

$$\mathrm{CV}^2_{\mathrm{uncorr}} = \frac{1}{\overline{k_{tl}}\,\overline{k_{tc}}\,\overline{n_D}} + \frac{1}{\overline{k_{tc}}\,\overline{n_D}}(CV^2_{k_{tl}} + 1) \quad (6)$$

where $\mathrm{CV}^2_{k_{tl}} = v_{k_{tl}}/\overline{k_{tl}}^2$, and $\mathrm{CV}^2_{k_{tc}} = v_{k_{tc}}/\overline{k_{tc}}^2$. Using these equations, we can evaluate the amplitude of the expression noise given the mean values $\overline{n_D}$, $\overline{k_{tc}}$, and $\overline{k_{tl}}$. The fluctuations in the transcription and translation rates among individual vesicles, $\mathrm{CV}^2_{k_{tc}}$ and $\mathrm{CV}^2_{k_{tl}}$, will be estimated by fitting these equations to the experimental data. In a later section, we experimentally measure these mean values and discuss the contributions of each term. For the mRNA start reaction, we obtain

$$\mathrm{CV}^2_{\mathrm{corr}} = \frac{1}{\overline{k_{tl}}\,\overline{n_m}} + \frac{1}{\overline{n_m}}(\mathrm{CV}^2_{k_{tl}} + 1) + 2\mathrm{CV}^2_{k_{tl}} \quad (7)$$

$$\mathrm{CV}^2_{\mathrm{uncorr}} = \frac{1}{\overline{k_{tl}}\,\overline{n_m}} + \frac{1}{\overline{n_m}}(\mathrm{CV}^2_{k_{tl}} + 1) \quad (8)$$

In this case, the first and second terms in $\mathrm{CV}^2_{\mathrm{corr}}$ and $\mathrm{CV}^2_{\mathrm{uncorr}}$ represent the noise in translation (i) and the noise in mRNA encapsulation amplified by translation (ii), respectively; these two terms are common to the two equations because these events are not correlated between the two FPs. The only difference is the third term in $\mathrm{CV}^2_{\mathrm{corr}}$, which arises from the fluctuation in the translation rate (iv) that globally affects the FP synthesis.

In the practical experiment, the abundances of YFP and BFP, as well as that of their transcripts (mRNAs), are not the same. To take these biases into account, we introduced the coefficients α_y and α_b for deviation from the mean $\overline{k_{tc}}$ and β_y and β_b for the deviation from the mean $\overline{k_{tl}}$. The full version of the equations for $\mathrm{CV}^2_{\mathrm{corr}}$ and $\mathrm{CV}^2_{\mathrm{uncorr}}$ are described in the Supporting Information (eqs S1, S2, S5, S6), which are used to analyze the experimental data). However, the factors from these coefficients are on the order of 1; thus, the contributions of the reaction steps to the correlated and uncorrelated noises can be essentially understood with the above equations.

Comparison with the Model. Equations 5−8 predict the amplitude of the correlated and uncorrelated noise components for a set of mean values in the elemental steps. To compare this prediction with the experimental result (Figure 4), the mean values were evaluated as follows. In the DNA start reaction, the number of DNA molecules in a vesicle, $\overline{n_D}$, was estimated as the DNA concentration (molecules/fL) multiplied by the volume (fL) of the vesicle of interest. The number of mRNA molecules for each FP in a vesicle, $\overline{n_{m,y}}$ and $\overline{n_{m,b}}$, was estimated using the mRNA concentration measured when conducting the same reaction in a test tube; the concentration was measured using the reverse transcription quantitative polymerase chain reaction (RT-qPCR) (Supporting Information Figure S8). The number of FPs, $\overline{n_{p,y}}$ and $\overline{n_{p,b}}$, was the average number of FPs in the flow cytometer measurement. Hence, the transcription and translation rates in eqs 5−8 were derived to be $\overline{k_{tc}} = \overline{n_m}/\overline{n_D}$ and $\overline{k_{tl}} = \overline{n_p}/\overline{n_m}$. $\overline{n_D}$, $\overline{n_m}$, and $\overline{n_p}$ for vesicles having ∼6000 synthesized FPs and are listed in Table 1. For example, in the expression from the 0.33 nM DNA ($V \sim 35$ fL population) condition, approximately 1.8×10^3 mRNA molecules were transcribed from approximately 7 plasmid DNA molecules; therefore, $\overline{k_{tc}}$ was 2.6×10^2 mRNA/DNA during the 240 min incubation. Similarly, approximately 6.2×10^3 FPs were translated from approximately 1.8×10^3 mRNA molecules; thus, $\overline{k_{tl}}$ was 2.8 FP/mRNA. Substituting these values into eqs 5 and 6 (eqs S1 and S2 in practice) produces $\mathrm{CV}_{\mathrm{corr}} = 0.58$ and $\mathrm{CV}_{\mathrm{uncorr}} = 0.028$ if we assume $\mathrm{CV}^2_{k_{tl}} = \mathrm{CV}^2_{k_{tc}} = 0$. In contrast, the corresponding values in the experiment were $\mathrm{CV}_{\mathrm{corr}} = 0.64$ and $\mathrm{CV}_{\mathrm{uncorr}} = 0.23$ (Figure 4a). Thus, the model predicted the correlated noise well but underestimated the uncorrelated noise.

Next, we asked whether the fluctuations in transcription and translation activities among vesicles, that is, $\mathrm{CV}_{k_{tc}}$ and $\mathrm{CV}_{k_{tl}}$, respectively, could explain this mismatch in the uncorrelated noise. The fluctuation in the transcription activity $\mathrm{CV}_{k_{tc}}$ does not contribute to eq 6. In contrast, the fluctuation in the translation rate $\mathrm{CV}_{k_{tl}}$ contributes to the amplification of the Poisson noise in transcription; thus, $\mathrm{CV}_{k_{tl}}$ may explain the seemingly larger uncorrelated noise. However, in eq 5, we find that assuming a large $\mathrm{CV}_{k_{tl}}$ also increases the correlated noise (the last term $2\mathrm{CV}^2_{k_{tl}}$) to a larger extent because the translation activity in a vesicle affects the translation of both FPs. Thus, another assumption is missing in the model. Among the three key substances in the reaction, DNA, mRNA, and FP, mRNA is generally the most unstable molecule. In addition to its intrinsic instability as a chemical structure, mRNA often has multiple secondary structures that may hinder ribosome binding and translation activity. To take this effect into account, we introduce the active ratio of mRNA, γ_{RNA}, into the model. This factor indicates that only a fraction of the total mRNA measured by RT-qPCR is active, that is, $\overline{n_m} = \gamma_{\mathrm{RNA}}\cdot\overline{n_m} = \overline{n_D}\cdot\gamma_{\mathrm{RNA}}\cdot\overline{k_{tc}}$ and $\overline{k_{tl}} = \overline{k_{tl}}/\gamma_{\mathrm{RNA}}$, where $\overline{n_m}$ and $\overline{k_{tl}}$ are the number of active mRNA and the compensated activity of translation, respectively. After introducing this variable into eqs 5−8, we searched a set of global parameters, γ_{RNA}, $\mathrm{CV}_{k_{tc}}$, and $\mathrm{CV}_{k_{tl}}$, that optimize the fitting to all of the experimental data. The result is shown in Figure 4 as bold solid lines. With $\gamma_{\mathrm{RNA}} \approx 0.03$, $\mathrm{CV}_{k_{tc}} \approx$

dx.doi.org/10.1021/sb500249g | ACS Synth. Biol. 2015, 4, 566−576

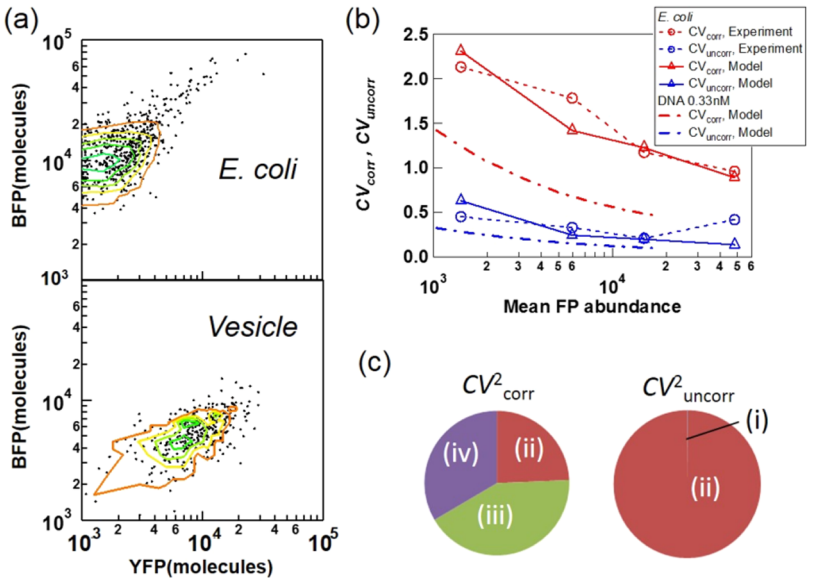

Figure 5. Gene expression noise measured in *E. coli*. (a) Correlated and uncorrelated noises in CV for the expression of YFP and BFP in *E. coli* induced by various IPTG concentrations. Experimental result was best fitted with the parameters $\gamma_{RNA} = 1$ and $CV_{k_{tl}} = 0.33$. Noises in 0.33 nM DNA start reaction, in which number of DNA n_D is nearly the same, are also shown. Vertical dotted line shows the mean FP abundance ~6000, at which the measured mean values are listed in Table 2. (b) Relative contributions to the noise explained in eqs 5 and 6 in CV^2 for *E. coli* expressing ~6000 FP. (i) The Poisson noise in translation, (ii) the Poisson noise in transcription, (iii) the Poisson noise in DNA encapsulation, and (iv) the vesicle-to-vesicle variation in the translation rate.

Table 2. List of Average Values in the Gene Expression in *E. coli* Determined by Fitting to the Model Equations[a]

	V (fL)	n_D	$\gamma_{RNA}n_m$	n_p	$\gamma_{RNA}k_{tc}$	α_y	α_b	k_{tl}/γ_{RNA}	β_y	β_b
DNA 0.33 nM	35.0	6.9	54	6315	7.75	0.46	2.16	117.6	2.84	0.35
E. coli (IPTG 15 μM)	4.0	8.1	7	5957	0.89	0.54	1.85	828.4	0.76	1.32

[a] γ_{RNA} for in liposome reaction (DNA 0.33 nM) is 0.03, whereas γ_{RNA} for *E. coli* was 1.

0, and $CV_{k_{tl}} \approx 0.2$, the model showed good agreement with the experimental data.

From this fitting result, we can characterize the noise in the artificial cell. The contribution of each term in eqs 5−8 is shown in the pie chart in the inset (Figure 4). In the DNA start reaction, the CV^2_{corr} (Figure 4a, left) is mainly dominated by the fluctuation in the number of encapsulated DNA molecules, which contributes $2/\overline{n_D}(CV^2_{k_{tl}} + 1)$, because $\overline{n_D}$ is the lowest compared to $\overline{n_m}$ and $\overline{n_p}$. The noise components from transcription (ii) and vesicle-to-vesicle variation (iv) had small but modest contributions to CV^2_{corr}. In turn, the fluctuation in the plasmid DNA did not affect the uncorrelated noise because the FP genes were located on the same plasmid molecules. Thus, CV^2_{uncorr} is mostly from the noise in the transcription step, which contributes $1/\overline{k_{tc}}\overline{n_D}(CV^2_{k_{tl}} + 1)$ (Figure 4a, right). This term becomes observable only when the transcription activity is small for fixed $\overline{n_D}$; this condition was met when $\gamma_{RNA} \approx 0.03$. In the mRNA start reaction, CV^2_{corr} (Figure 4b, left) was mainly dominated by the vesicle-to-vesicle fluctuation in the translation rate (iv), which contributes $2CV^2_{k_{tl}}$, whereas the noise in the number of encapsulated RNA molecules (ii) had a small contribution. Because the vesicle-to-vesicle variation term (iv) does not depend on the other parameters, the profile of the correlated noise was relatively flat (CV_{corr} = 0.3−0.5) over the range of mean FP abundance in both the experimental measurement and the theoretical prediction. The CV^2_{uncorr} in the mRNA start reaction (Figure 4b, right) was dominated by the noise from the mRNA number in a manner similar to that of CV_{uncorr} in the DNA start reaction. The Poisson noise in the translation (i) step had a negligible contribution in all cases because the fluctuation was mainly generated in the upstream reaction steps.

Comparison with *E. coli*. Next, we compared the expression noise in the artificial cell with that in the simple biological cell. We measured the expression of the dual FPs in *E. coli* using the same plasmid DNA as for the *in vitro* system. The plasmid DNA was transformed into *E. coli* strain *JM109* (DE3), which was repeatedly cultured in M63 medium until a certain growth rate was reached. This strain was stored at −80 °C in 30% glycerol medium. For preculture, the frozen cells were inoculated in M63 without inducer and cultured at 37 °C overnight. For the expression of the FPs, the cells were transferred into M63 with various IPTG concentrations (0, 15, 20, and 30 μM) and were incubated. The abundances of the FPs were measured via FCS at various time periods during the incubation. The data in which the FP synthesis reached a plateau (22 h) were analyzed. The scatterplot of the synthesized YFP and BFP, with a mean FP ~ 6000, is shown in Figure 5a. Note that, this time, the protein abundances are on a logarithmic scale because the *E. coli* population contained cells with an extremely high expression level ($n_{p,b} \sim 10^5$). The same scatterplot for the artificial cell with 0.33 nM DNA (corresponding to ~7 plasmid/vesicle, close to the value for *E. coli*) is shown for comparison.

For model-based predictions of the noise, the average number of plasmid DNAs was measured by qPCR, and the

dx.doi.org/10.1021/sb500249g | *ACS Synth. Biol.* 2015, 4, 566−576

value was ~8 plasmid/cell regardless of the IPTG concentration. The amount of each type of mRNA was measured by RT-qPCR (Supporting Information Figure S9), and the value was dependent on the IPTG concentration (i.e., expression level). For instance, the mean mRNA number was 7 mRNA/cell at 15 μM IPTG, when the mean FP was approximately 6000 (Table 2). The small copy number of mRNA is likely due to the rapid degradation *in vivo*. Using these numbers, we analyzed the correlated and uncorrelated noise. In FCS, the forward scattering signal (FSS) in known to reflect the size of *E. coli*, but we confirmed that neither the mean nor the variance of the FPs was dependent on the FSS (Supporting Information Figure S10). Thus, we used the most frequent fraction in the FSS distribution for analysis. The noise components in CV that are derived from the experiment are shown with circular symbols in Figure 5b. In *E. coli*, CV_{corr} was approximately twice that in the artificial cell (shown as broken lines), but CV_{uncorr} was nearly the same. CV_{corr} and CV_{uncorr} were fitted by eqs 5 and 6, using the average values listed in Table 2, with free variables γ_{RNA}, $CV_{k_{tc}}$, and $CV_{k_{tl}}$. The fitting result is shown as triangular symbols in Figure 5b. Here, the noise exhibited in *E. coli* was best fitted with $\gamma_{RNA} \approx 1$, $CV_{k_{tc}} \approx 0$ and $CV_{k_{tc}} \approx 0.33$. This result indicates that the majority of the mRNA was active *in vivo*, which is consistent with literature.[5] The variation in the translation activity, $CV_{k_{tl}}$, was estimated to be approximately 1.5-fold greater than that in the artificial cell. Because the *E. coli* and the artificial cell at $\overline{n}_p \approx 6000$ contained nearly the same number of plasmid DNAs, the higher CV_{corr} in *E. coli* is caused by the greater noise from the small transcription activity that appears as term (ii) and the higher level of cell-to-cell variation in the translation rate that appears as term (iv) (Figure 5c). In contrast, the similarity in CV_{uncorr} indicates that the noise from the stochasticity in the transcription steps was common to the *in vivo* and artificially reconstituted systems because this noise is inherent to the system and unavoidable.

Discussion. In this work, we studied the expression noise in an artificial cell, which contained an *in vitro* gene expression system in a model cell membrane. The source of the correlated noise was mainly the fluctuation in the number of encapsulated DNA molecule, which is the most upstream component in the reaction cascade. This fact also indicates that the DNA molecule is 100% active even at the single molecular level in vesicles, which is consistent with our previous reports.[47] The vesicle-to-vesicle variation in the transcription and translation rates that act globally in the reaction was relatively small, indicating that vesicles act as uniform reaction containers that are inert to the reaction. There has been an extensive discussion about behavior of the metabolic reaction might deviate significantly from that in larger compartment, possible due to the variation in the number of reaction components and the influence from the lipid membrane.[36,48−50] However, our result indicates it is not the case in the microscale vesicles, in which the every component in PURE system has more than 100 molecules in 10 fL volume (Supporting Information Table S2).

In contrast, the uncorrelated noise was unexpectedly large if we assumed that all of the mRNA molecules, which were measured by the RT-qPCR, were active. Because the uncorrelated noise mainly reflects the independent fluctuation in the transcription process, the model predicts that the mRNA molecules are only partly active, and the small number of transcripts per DNA contributes to the uncorrelated noise. To date, there is no direct evidence for a low active ratio for the mRNA synthesized in an artificially reconstructed transcription system; however, a low active ratio is likely because mRNA is the most unstable biopolymer in the cascade. In comparison to *E. coli*, the artificial cell had less correlated noise. The greater amplitude of the correlated noise in *E. coli* was mainly from the larger cell-to-cell variation in the translation activity. In fact, the distribution of FPs in *E. coli* had a fat tail, reflecting the presence of a cell with an extraordinarily high expression level. This observation could be attributed to the variation in the growth rate of the cell[10] and/or in the degradation of proteins, whereas both effects are negligible in the artificial cell. In contrast, the order of the uncorrelated noise was similar in the two systems because transcription stochasticity is unavoidable.

In addition to the above-mentioned differences that are on the order of a few fold, our result revealed that the simple artificial cell had roughly the same level of correlated and uncorrelated noise as that in a living cell (*E. coli*). This result indicates that during the course of evolution from the extremely primitive cell form to the prokaryote, the cell did not have to acquire specific machinery for generating and regulating noise because the noise was intrinsically present in the cell, which functioned as a minute microreactor. Consequently, this finding suggests that cells could have utilized the existence of noise for evolution, differentiation, and adaptation from the very beginning.

METHODS

Construction and Preparation of the Plasmid. The utilized YFP and BFP were mVenus (Venus YFP with monomerizing A206 K mutation) and TagBFP (Evrogen), respectively. First, the sequences of the YFP or BFP genes were respectively inserted into the *nde1-Xho1* site in pET21a using the In-Fusion method (Takara Bio Inc.). These two plasmid DNAs were called pET_YFP and pET_BFP, and they were fused with a His tag at the C terminal for protein purification. Second, the sequence of the BFP gene, which included the T7 promoter and T7 terminator, was amplified from pET_BFP and inserted into the *lacI* site of pET_YFP using the In-Fusion method. This final plasmid having both the YFP and BFP genes was called pET-YFP_BFP. The constructed plasmid was transformed into competent *E. coli* cells (XL10-Gold, Stratagene), which were cultured for amplification. The amplified plasmid was purified using a QIAfilter Plasmid Midi Kit (Qiagen). The mRNA was prepared using an *in vitro* transcription T7 kit (Takara Bio Inc.). The plasmid (50 μg), which was the pET-YFP_BFP prepared above, was added to an 800-μL mixture consisting of 40 mM Tris-HCl (pH 8.0), 8 mM $MgCl_2$, 5 mM DTT, 2 mM spermidine, 0.4 mM NTPs, and 20 μg of T7 RNA polymerase, and the mixture was incubated at 37 °C for 5 h. The RNA was purified using an RNeasy Mini Kit (Qiagen) in accordance with the manufacturer's instructions. The DNA remaining in the mixture was digested with recombinant DNase I (RNase-free, Takara Bio Inc.), and the mRNA was purified using the RNeasy Mini kit (Qiagen). The DNA and mRNA concentrations were determined from the absorbance at 260 nm.

***In Vitro* Transcription and Translation System.** The *in vitro* transcription and translation system was a modified version of the PURE system[51] described in previous studies.[52,53] T7 polymerase and the other PURE system protein components were all purified from *E. coli* in our laboratory, and the composition was described previously.[47] For the reaction in the test tube, the template plasmid DNA or

dx.doi.org/10.1021/sb500249g | ACS Synth. Biol. 2015, 4, 566−576

mRNA was added to the PURE system and was supplemented with 1 μM transferrin-Alexa Fluor 647 conjugate (TA647; Invitrogen) and 0.2 unit/mL RNasin (Promega). The synthesis of the FPs, which were incubated at 37 °C, was monitored using a real-time qPCR system (Mx3005P, Agilent Technologies, Inc.). The concentration of mRNA in the PURE system reaction mixture was determined as follows. The reaction mixture was sampled and immediately diluted 10 000 times with RNase-free water and stored at 0 °C to stop the reaction and RNA degradation. Next, the amount of each mRNA (YFP and BFP) was measured by the RT-qPCR method using a PrimeScript One Step RT-PCR Kit (Takara Bio Inc.). For each gene, a forward primer (qRTPCR-YFP-F: CTGGTGGACAGCAAATGGGTCG and qRTPCR-BFP-F: GCACCGTGGACAACCATCACTTC) was used. The same reverse primer, qRTPCR-pET-R: CCTTTCGGGCTTTGTTAGCAGCCG, was used to measure the YFP and BFP mRNA.

Preparation of Cell-Seized Vesicles for Encapsulating the *In Vitro* Transcription and Translation System. The giant unilamellar vesicles that encapsulated the PURE system were prepared using the water-in-oil emulsion transfer method, as described previously.[39,46] In short, 1-palmitoyl-2-oleoyl-*sn*-glycero-3-phosphocholine (POPC, from Avanti Polar Lipids) and cholesterol (Nacalai Tesque) were dissolved in liquid paraffin (Wako Pure Chemical Industries, Ltd.) at 5 mg/mL. Aliquots of 20 μL of the PURE system solution, which was prepared above, were added to the 250 μL of liquid paraffin. This solution also contained transferrin-Alexa Fluor 647 conjugate (TA647; Invitrogen) as a volume marker. This mixture was vortexed for 30 s to form w/o emulsions that were then equilibrated on ice for 10 min. Then, 200 μL of the emulsion was placed gently on top of 200 μL of the outer solution and centrifuged at 18000*g* and 4 °C for 30 min. The outer solution consisted of the small molecular weight components of the PURE system (2.0 mM each amino acid, 2 mM ATP, 1.3 mM GTP, 0.67 mM CTP and UTP, 3.7 mM spermidine, 45 mM creatine phosphate, 1.5 mM dithiothreitol (DTT), 0.02 μg/μL N5-formyl-5,6,7,8-tetrahydropteroyl-L-glutamic acid (FD), 282 mM potassium glutamate, 15.4 mM $Mg(OAc)_2$, and 100 mM HEPES). The sedimented vesicles were collected through a hole that was opened in the bottom of the tube.

Gene Expression in Cell-Seized Vesicles and FCS Measurement. The gene expression reaction (synthesis of FPs) encapsulated in the cell seized vesicles was initiated by incubating the vesicles suspension at 37 °C. Small aliquots were sampled every 30 min, and after dilution with the isotonic buffer (100 mM HEPES-KOH, pH 7.6, 15.4 mM $Mg(OAc)_2$, and 417 mM potassium glutamate), samples were measured using FCS. The FCS intensities of three fluorescence signals, that is, YFP, BFP, and TA647 were measured, and these intensities were converted to the number of protein molecules using calibration curves.[39,46] Practically, YFP was excited with a solid state laser (488 nm), and the emission was detected through a 530 ± 15 nm band-pass filter. BFP was excited with a violet solid state laser (405 nm), and the emission was detected through a 450 ± 10 nm band-pass filter. The number of FPs was obtained using the equations $FI_{YFP} \times 30.3$ and $FI_{BFP} \times 15.9$. TA647 was excited with a HeNe laser (633 nm), and the emission was detected through a 660 ± 10 nm band-pass filter. The fluorescence intensity was converted to the volume using the equation $FI_{TA647} \times 0.00398 = V$ (fL). In each measurement, 100 000 data points were obtained and used for the post analysis.

Gene Expression in *E. coli*. Competent cells (20 μL) (JM109 (DE3)) and 1 μL of plasmid DNA were mixed and incubated on ice for 10 min. Then, the mixture was heated in a 42 °C water bath for 30 s and then incubated on ice for 2 min. After the addition of 180 μL of LB medium, the cells were incubated at 37 °C for 30 min. Next, the transformed cells were selected by culturing on an LB plate with 5 μg/mL ampicillin at 37 °C overnight. The transformed cells were cultured in M63 medium, which consisted of 62 mM K_2HPO_4, 39 mM KH_2PO_4, 15 mM $(NH_4)_2SO_4$, 2 μM $FeSO_4 \cdot 7H_2O$, 15 μM thiamine hydrochloride, 203 μM $MgSO_4 \cdot 7H_2O$, and 22 mM glucose until a certain growth rate was reached. This strain was stored at −80 °C in 30% glycerol medium. For preculture, frozen cells were inoculated in M63 without inducer and cultured at 37 °C overnight. For induction of the expression of FPs, the cells were transferred in M63 with various IPTG concentrations (0, 15, 20, and 30 μM). The amount of YFP and BFP in the individual cells were measured by FCS with the same protocol as for the cell-sized vesicles after diluting the sample with M63 medium.

Measurement of DNA and mRNA in *E. coli*. The copy numbers of the plasmid DNA and the mRNA molecules in *E. coli* were determined as follows. After incubation, the concentration of *E. coli* was determined using FCS (FACS Aria, BD). Based on this value, several 10^7 cells were collected. Plasmid DNA was extracted and purified with a Miniprep Kit (Qiagen) and was measured by the qPCR method (SYBR Green, Takara) with two primers (forward primer: GGTATGGCTAGCATGACTGGTG and reverse primer CTCCTTTCAGCAAAAAACCCCTCAAGACCC). The mRNA was extracted and purified with RNeasy (Qiagen). Then, each mRNA (YFP and BFP) was measured by the RT-qPCR method with the same protocol as used for the *in vitro* transcription and translation system.

■ ASSOCIATED CONTENT

Supporting Information

Supporting equations and figures. This material is available free of charge via the Internet at http://pubs.acs.org.

■ AUTHOR INFORMATION

Corresponding Author

*Tel: 81-6-6879-4171. Fax: 81-6-6879-7433. E-mail: Yomo@ist.osaka-u.ac.jp.

Author Contributions

K.N., S.T., and T.Y. conceived the project. K.N. designed and conducted the experiments. T.S. constructed the theoretical model. K.N. and H.S conducted the analysis. The paper was written by H.S. and edited by all of the coauthors.

Notes

The authors declare no competing financial interest.

■ ACKNOWLEDGMENTS

We thank Dr. Yasuaki Kazuta, Ms. Hitomi Komai, and Ms. Tomomi Sakamoto for producing the PURE system. This research was supported in part by the "Global Centers of Excellence Program" of the Ministry of Education, Culture, Sports, Science, and Technology, Japan.

REFERENCES

(1) Elowitz, M. B., Levine, A. J., Siggia, E. D., and Swain, P. S. (2002) Stochastic gene expression in a single cell. *Science 297*, 1183−1186.
(2) Ozbudak, E. M., Thattai, M., Kurtser, I., Grossman, A. D., and van Oudenaarden, A. (2002) Regulation of noise in the expression of a single gene. *Nat. Genet. 31*, 69−73.
(3) Yu, J., Xiao, J., Ren, X. J., Lao, K. Q., and Xie, X. S. (2006) Probing gene expression in live cells, one protein molecule at a time. *Science 311*, 1600−1603.
(4) Cai, L., Friedman, N., and Xie, X. S. (2006) Stochastic protein expression in individual cells at the single molecule level. *Nature 440*, 358−362.
(5) Taniguchi, Y., Choi, P. J., Li, G. W., Chen, H. Y., Babu, M., Hearn, J., Emili, A., and Xie, X. S. (2010) Quantifying *E. coli* proteome and transcriptome with single-molecule sensitivity in single cells. *Science 329*, 533−538.
(6) Raser, J. M., and O'Shea, E. K. (2004) Control of stochasticity in eukaryotic gene expression. *Science 304*, 1811−1814.
(7) Eldar, A., and Elowitz, M. B. (2010) Functional roles for noise in genetic circuits. *Nature 467*, 167−173.
(8) Raj, A., and van Oudenaarden, A. (2008) Nature, nurture, or chance: Stochastic gene expression and its consequences. *Cell 135*, 216−226.
(9) Balazsi, G., van Oudenaarden, A., and Collins, J. J. (2011) Cellular decision making and biological noise: From microbes to mammals. *Cell 144*, 910−925.
(10) Tsuru, S., Ichinose, J., Kashiwagi, A., Ying, B. W., Kaneko, K., and Yomo, T. (2009) Noisy cell growth rate leads to fluctuating protein concentration in bacteria. *Phys. Biol. 6*, 036015.
(11) Segre, D., and Lancet, D. (2000) Composing life. *Embo. Rep. 1*, 217−222.
(12) Szostak, J. W., Bartel, D. P., and Luisi, P. L. (2001) Synthesizing life. *Nature 409*, 387−390.
(13) Forster, A. C., and Church, G. M. (2006) Towards synthesis of a minimal cell. *Mol. Syst. Biol. 2*, 45 DOI: 10.1038/msb4100090.
(14) Luisi, P. L. (2007) Chemical aspects of synthetic biology. *Chem. Biodivers. 4*, 603−621.
(15) Stano, P., and Luisi, P. L. (2010) Achievements and open questions in the self-reproduction of vesicles and synthetic minimal cells. *Chem. Commun. 46*, 3639−3653.
(16) Jewett, M. C., and Forster, A. C. (2010) Update on designing and building minimal cells. *Curr. Opin. Biotechnol. 21*, 697−703.
(17) Oberholzer, T., Nierhaus, K. H., and Luisi, P. L. (1999) Protein expression in liposomes. *Biochem. Biophys. Res. Commun. 261*, 238−241.
(18) Yu, W., Sato, K., Wakabayashi, M., Nakaishi, T., Ko-Mitamura, E. P., Shima, Y., Urabe, I., and Yomo, T. (2001) Synthesis of functional protein in liposome. *J. Biosci. Bioeng. 92*, 590−593.
(19) Nomura, S., Tsumoto, K., Hamada, T., Akiyoshi, K., Nakatani, Y., and Yoshikawa, K. (2003) Gene expression within cell-sized lipid vesicles. *ChemBioChem 4*, 1172−1175.
(20) Noireaux, V., and Libchaber, A. (2004) A vesicle bioreactor as a step toward an artificial cell assembly. *Proc. Natl. Acad. Sci. U.S.A. 101*, 17669−17674.
(21) Oberholzer, T., Albrizio, M., and Luisi, P. L. (1995) Polymerase Chain-Reaction in Liposomes. *Chem. Biol. 2*, 677−682.
(22) Fischer, A., Franco, A., and Oberholzer, T. (2002) Giant vesicles as microreactors for enzymatic mRNA synthesis. *ChemBioChem 3*, 409−417.
(23) Mansy, S. S., Schrum, J. P., Krishnamurthy, M., Tobe, S., Treco, D. A., and Szostak, J. W. (2008) Template-directed synthesis of a genetic polymer in a model protocell. *Nature 454*, 122−125.
(24) Kita, H., Matsuura, T., Sunami, T., Hosoda, K., Ichihashi, N., Tsukada, K., Urabe, I., and Yomo, T. (2008) Replication of genetic information with self-encoded replicase in liposomes. *ChemBioChem 9*, 2403−2410.
(25) Hanczyc, M. M., Fujikawa, S. M., and Szostak, J. W. (2003) Experimental models of primitive cellular compartments: Encapsulation, growth, and division. *Science 302*, 618−622.
(26) Zhu, T. F., and Szostak, J. W. (2009) Coupled growth and division of model protocell membranes. *J. Am. Chem. Soc. 131*, 5705−5713.
(27) Paleos, C. M., Tsiourvas, D., and Sideratou, Z. (2011) Interaction of vesicles: Adhesion, fusion, and multicompartment systems formation. *ChemBioChem 12*, 510−521.
(28) Schrum, J. P., Zhu, T. F., and Szostak, J. W. (2010) The origins of cellular life. *Cold Spring Harb. Perspect Biol. 2*, a002212.
(29) Kurihara, K., Tamura, M., Shohda, K., Toyota, T., Suzuki, K., and Sugawara, T. (2011) Self-reproduction of supramolecular giant vesicles combined with the amplification of encapsulated DNA. *Nat. Chem. 3*, 775−781.
(30) Zhu, T. F., Adamala, K., Zhang, N., and Szostak, J. W. (2012) Photochemically driven redox chemistry induces protocell membrane pearling and division. *Proc. Natl. Acad. Sci. U.S.A. 109*, 9828−9832.
(31) Terasawa, H., Nishimura, K., Suzuki, H., Matsuura, T., and Yomo, T. (2012) Coupling of the fusion and budding of giant phospholipid vesicles containing macromolecules. *Proc. Natl. Acad. Sci. U.S.A. 109*, 5942−5947.
(32) Briers, Y., Walde, P., Schuppler, M., and Loessner, M. J. (2012) How did bacterial ancestors reproduce? Lessons from L-form cells and giant lipid vesicles. *Bioessays 34*, 1078−1084.
(33) Mercier, R., Kawai, Y., and Errington, J. (2013) Excess membrane synthesis drives a primitive mode of cell proliferation. *Cell 152*, 997−1007.
(34) Lasic, D. D. (1988) The mechanism of vesicle formation. *Biochem. J. 256*, 1−11.
(35) Walde, P., Cosentino, K., Engel, H., and Stano, P. (2010) Giant vesicles: Preparations and applications. *ChemBioChem 11*, 848−865.
(36) Pereira de Souza, T., Steiniger, F., Stano, P., Fahr, A., and Luisi, P. L. (2011) Spontaneous crowding of ribosomes and proteins inside vesicles: A possible mechanism for the origin of cell metabolism. *Chembiochem 12*, 2325−2330.
(37) Saito, H., Kato, Y., Le Berre, M., Yamada, A., Inoue, T., Yosikawa, K., and Baigl, D. (2009) Time-resolved tracking of a minimum gene expression system reconstituted in giant liposomes. *ChemBioChem 10*, 1640−1643.
(38) Karig, D. K., Jung, S. Y., Srijanto, B., Collier, C. P., and Simpson, M. L. (2013) Probing cell-free gene expression noise in femtoliter volumes. *ACS Synth. Biol. 2*, 497−505.
(39) Nishimura, K., Matsuura, T., Sunami, T., Suzuki, H., and Yomo, T. (2012) Cell-free protein synthesis inside giant unilamellar vesicles analyzed by flow cytometry. *Langmuir 28*, 8426−8432.
(40) Nishikawa, T., Sunami, T., Matsuura, T., and Yomo, T. (2012) Directed evolution of proteins through *in vitro* protein synthesis in liposomes. *J. Nucleic Acids 2012*, 923214.
(41) Fujii, S., Matsuura, T., Sunami, T., Kazuta, Y., and Yomo, T. (2013) *In vitro* evolution of α-hemolysin using a liposome display. *Proc. Natl. Acad. Sci. U.S.A. 110*, 16796−16801.
(42) Swain, P. S., Elowitz, M. B., and Siggia, E. D. (2002) Intrinsic and extrinsic contributions to stochasticity in gene expression. *Proc. Natl. Acad. Sci. U.S.A. 99*, 12795−12800.
(43) Paulsson, J. (2004) Summing up the noise in gene networks. *Nature 427*, 415−418.
(44) Hase, M., Yamada, A., Hamada, T., Baigl, D., and Yoshikawa, K. (2007) Manipulation of cell-sized phospholipid-coated microdroplets and their use as biochemical microreactors. *Langmuir 23*, 348−352.
(45) Pautot, S., Frisken, B. J., and Weitz, D. A. (2003) Production of unilamellar vesicles using an inverted emulsion. *Langmuir 19*, 2870−2879.
(46) Nishimura, K., Hosoi, T., Sunami, T., Toyota, T., Fujinami, M., Oguma, K., Matsuura, T., Suzuki, H., and Yomo, T. (2009) Population analysis of structural properties of giant liposomes by flow cytometry. *Langmuir 25*, 10439−10443.
(47) Hosoda, K., Sunami, T., Kazuta, Y., Matsuura, T., Suzuki, H., and Yomo, T. (2008) Quantitative study of the structure of multilamellar giant liposomes as a container of protein synthesis reaction. *Langmuir 24*, 13540−13548.

(48) de Souza, T. P., Stano, P., and Luisi, P. L. (2009) The minimal size of liposome-based model cells brings about a remarkably enhanced entrapment and protein synthesis. *ChemBioChem 10*, 1056−1063.
(49) Pantazis, Y., Katsoulakis, M. A., and Vlachos, D. G. (2013) Parametric sensitivity analysis for biochemical reaction networks based on pathwise information theory. *BMC Bioinformatics 14*, 311 DOI: doi:10.1186/1471-2105-14-311.
(50) Calviello, L., Stano, P., Mavelli, F., Luisi, P. L., and Marangoni, R. (2013) Quasi-cellular systems: Stochastic simulation analysis at nanoscale range. *BMC Bioinformatics 14*, S7 DOI: 10.1186/1471-2105-14-S7-S7.
(51) Shimizu, Y., Inoue, A., Tomari, Y., Suzuki, T., Yokogawa, T., Nishikawa, K., and Ueda, T. (2001) Cell-free translation reconstituted with purified components. *Nat. Biotechnol. 19*, 751−755.
(52) Matsuura, T., Kazuta, Y., Aita, T., Adachi, J., and Yomo, T. (2009) Quantifying epistatic interactions among the components constituting the protein translation system. *Mol. Syst. Biol. 5*, 297.
(53) Kazuta, Y., Adachi, J., Matsuura, T., Ono, N., Mori, H., and Yomo, T. (2008) Comprehensive analysis of the effects of *Escherichia coli* ORFs on protein translation reaction. *Mol. Cell. Proteomics 7*, 1530−1540.